Recycling, Divertor Parameters and SOL Transport for High Performance Discharges in the New JET

K. McCormick[1], J.Ehrenberg, A.Loarte, R.Monk[2], R.Simonini, J.Spence, M.Stamp, A.Taroni, G.Vlases

JET Joint Undertaking, Abingdon, Oxon., OX14 3EA, UK

1) Max-Planck-Institut für Plasmaphysik, EURATOM Association, Garching, Germany

2) Royal Holloway College, University of London, Surrey, TW20 OEX, UK

1. Introduction:

The early stages of hot-ion mode operation with the new JET yielded, in marked contrast to the ELM-free behavior of the previous configuration, high performance H-modes with type I ELMs evoking lower D-D reaction rates (R_{DD}) in combination with higher recycling signals. Since it is known high recycling is deleterious to H-mode quality [1], this paper examines the relationship between recycling signals and R_{DD} for 1991 (graphite walls and upper dump plates, open divertor) and the present campaign 1994/95 (MkI pumped divertor, CFC target plates, largely inconel walls). A calibrated D_α signal (DAV) measured along a vertical chord on the outer side of the x-point and not intersecting the divertor, and common to 1991-1995, is utilized. After documentation of experimental results, the transport code EDGE2D/NIMBUS is employed to interpret DAV in the sense of: 1) Is there a difference in recycling between 1991 and 1994/95, and 2) Do any of the 1994/95 divertor equilibria exhibit benefits over others in terms of recycling control of neutrals from the divertor to the main chamber?

2. Experimental Results

Configuration	SNU	SF	HFE	DNHF1
x-pt height [m]	0.084	0.284	0.132	0.126
flux exp. in	17.6	3.4	12.6	13.6
flux exp. out	15	2.5	8	10
shear at q95	4.4	3.25	3.6	3.75
upper tri.	0.51	0.19	0.21	0.28
Best Example	**#26087**	**#32823**	**#32919**	**#33643**
Volume [m3]	101	81	83	79
P_{NI} [MW]	14.9	18.5	18.2	18.5
W_{DIA} [MJ]	11.6	10	10.8	12.3
R_{DD} [s-1]	8.4×10^{16}	5.6×10^{16}	7.6×10^{16}	9.3×10^{16}
δt to limit [s]	1.35	1.08	1.09	1.30
δN_{etotal} and $\int\Phi_{pump}$, Φ_{gas} Φ_{beam} over 1st sec of NBI				
$\int\Phi_{epumpdt}$	0	-1.08	-1.38	-0.72
$\int\Phi_{egasdt}$	2.65×10^{21}	0	0	0.37
$\int\Phi_{ebeamdt}$	1.16	1.6	1.55	1.54
δN_{etotal}	1.44	1.68	1.84	2.0
$\delta N_e/\int_{beam}$	1.24	1.05	1.19	1.31

Table I: Magnetic geometry, plasma properties and global particle balances for the best high performance shots of each configuration.

Table I lists characteristics of the best 1991 Single Null Up (SNU) case as well as the best each of three divertor equilibria of 1994/95. SNU had a low x-point and high flux expansion. SF, HFE and DNHF1 of 1994/95 represent a chronological evolution from a high to low x-point, and from a low flux expansion upwards. There is also a progression in main plasma triangularity and edge shear, but the values remain below those of SNU. P_{NI}, while larger for 1994/95 does not produce a notable R_{DD} margin over 1991, partly due to the smaller plasma volume necessitated by the divertor structure. The particle balance at the end of the 1st sec. of NBI shows with the cryopump (1994/95) the change in electron inventory relative to those injected is roughly the same as in 1991.

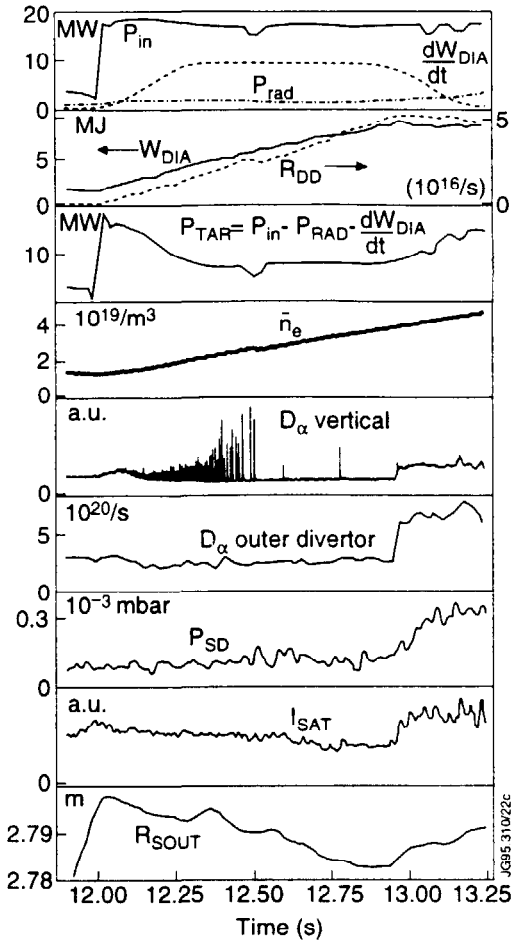

Fig.1: Time traces for global (top 4 boxes) and divertor parameters. The outer strike point (R_{sout}) drifts away from the probe over t=12->12.75 s, causing the decrease in I_{sat}. The "rollover" phase in R_{DD} and W_{dia} begins at t=12.95 sec. Shot #33641.

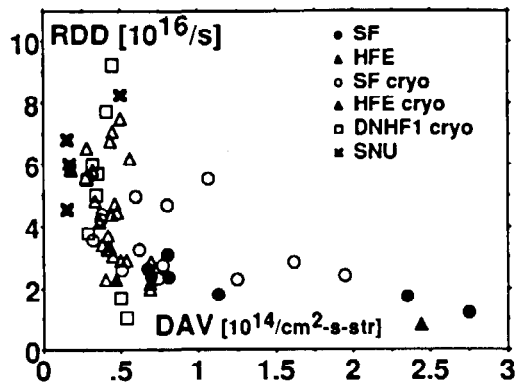

Fig. 2a: D-D reaction rate R_{DD} vs. the vertical D_α signal DAV (taken after the L-H transition) for 1991, and 1994-95 configurations with/without the cryopump.

The temporal behavior of recycling signals, in relationship to other divertor and global quantities during the transient ELM-free hot-ion H-mode phase is depicted in fig.1. The high P_{NI} ~ 17MW effects a calculated power to the target plate of only P_{tar} ~ 7MW, because of the large dW_p/dt (~ 9MW) but low total radiation (~ 1MW). R_{DD} and W_p rise linearly with time until the "rollover" at t ~ 52.95 sec. Both DAV and the outer target plate D_α signal (DAO) - along with the pressure of the sub-divertor volume P_{SD} and the saturation current to a target plate Langmuir probe - remain roughly constant after entering the ELM-free phase up to the rollover (ignoring the benign mini-ELMs). At the rollover, the increase in P_{target} is registered by all divertor diagnostics as an augmentation of ion flux. The fact that divertor properties remain relatively stable up to the rollover (while the core line density increases a factor of three!) is indicative that midplane values are not changing, a result familiar from ASDEX [2].

Fig. 2a plots the maximum R_{DD} attained vs. DAV, taken just after the L-H transition, for a number of discharges per equilibrium. The association of low R_{DD} <=> high DAVis self-evident only for very high recycling. As it stands, fig.2a demonstrates that the best R_{DD} values are not attained at the lowest DAV, either for 1991 or 1994/5. Fig.2b shows how the points of fig.2a are described by the regression:

$$R_{DD} \sim t(H)^{0.93\pm0.09}\, P_{NI}^{2.0\pm0.17}\ [s, MW],$$

where t(H) is the ELM-free period beginning at the L-H transition up to the event terminating high performance. The nearly linear time dependence is expected from fig.1. SNU (not used in the fit) is superior to 1994/5 as already noted in Table I. Normally, high performance shots are set up to minimize recycling, i.e. optimized wall conditioning, low target density, and no gas puff after NBI begin.

The points suffering heavy gas puffing before NBI (not used in the fit) illustrate the outcome, lying clearly below the norm. Furthermore, pumped-divertor shots are associated with higher R_{DD}, as are the configurations HFE and DNHF1 over SF.

Fig. 2c exemplifies that R_{DD} bears a relationship to DAV even at low recycling levels when examined in well-controlled circumstances. R_{DD} (normalized to P_{NI}^2, as well as to an average ELM-free time) goes up with decreasing DAVover eight, almost consecutive shots. The parallel enhancement in t(H) suggests this may be one mechanism by which R_{DD} is coupled to recycling, i.e. low recycling <=> low edge densities, leading to delay of the development of pressure-gradient-driven instabilities thought to end high performance[3,4]. The stability limit itself is determined by triangularity and edge shear, higher values yielding longer t(H) and thus higher R_{DD}. Hence, t(H) in the fit above implicitly represents the combined effects of reduced pressure gradients and higher stability.

The Langmuir probe data of table II illustrate that divertor plasmas of the hot-ion H-mode are typified by J_{sat} <10A/cm^2, n_{ed}<10^{19}/m^3 and T_{ed}~50-60eV when low recycling prevails. (Langmuir data exists for only one SF case - with high recycling.) The fall-off lengths when projected to the midplane are similar for all cases and quite small (λ_{Jsat} ~3-5mm). Using Langmuir data, computation of the power flow to the target plates, for an energy transmission factor γ=8 and T_i=T_e, accounts for less than 20% of P_{tar}. This discrepancy likely originates in the assumptions for T_i and γ, since the power balance is reasonable, i.e. the IR camera approximately validates P_{tar} [5], and since the probe saturation current values are quite compatible with measured D_α levels.

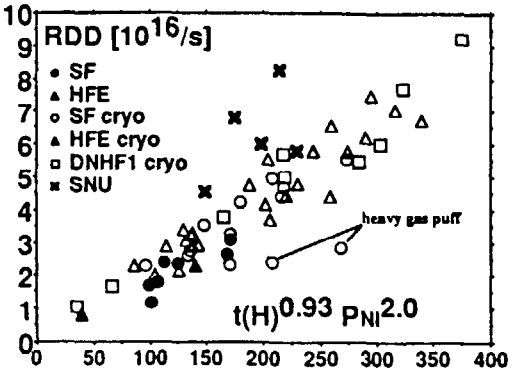

Fig. 2b: A fit to the points of fig. 2a using the ELM-free period t(H) and P_{NI}.

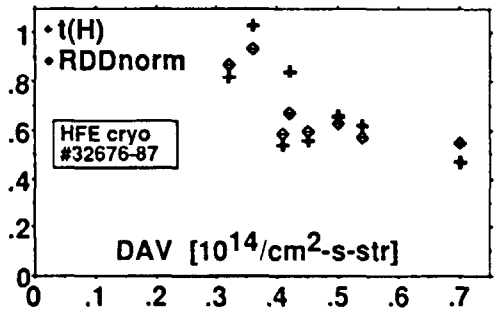

Fig.2c: Normalized R_{DD} and t(H) vs. DAV for a series of shots from fig. 2a.

Configuration	SF	HFE	DNHF1
Shot Number	#30917	#32919	#33643
J_{sat} [A/cm2]	30	7.9	7
λ [cm]	0.8 (0.32)	3.5 (0.44)	3.5 (0.35)
n_e [1013/cm3]	3.6	0.7	0.6
λ [cm]	0.9 (0.36)	4.2 (0.53)	4.0 (0.40)
T_e [eV]	30	52	56
λ [cm]	1.9 (0.76)	12 (1.50)	9.3 (0.93)

***Table II:** Outer target plate Langmuir probe data for hot-ion H-modes of Mkl. T_i=T_e is assumed here in the evaluation of n_e. () gives λ projected to the outer midplane.*

Configuration		SNU	SF	HFE	DNHF1
DAH	expt.	0.6	1.4	1.1	1.1
[1013]	code	0.5	0.9	0.33	0.63
DAV	expt.	4.4	7.5	5	6.6
[1013]	code	2.5	8.9	4.2	3.7
DAT	expt.		118	100	96
[1013]	code		146	116	119
Φ_{sol}	code	7.6x1021	13	8	7.9
S_{ion}	code	5.3x1021	6	3.9	4.1

***Table III:** Comparison of experimental-(best R_{DD} cases of Table I) and code-calculated D_α signals. Predicted neutral flux to the main SOL, and ionizations inside the separatrix.*

3. EDGE2D/NIMBUS Modelling of the Configurations and Comparison to Experiment

Considering the measured T_{ed}~50eV and power balance, the upstream power inputs to the code are taken as P_e=1MW, P_i=5MW. Such a power splitting is not inconsistent with core transport analysis [6], and also compatible with past modelling efforts [7]. Further conditions required to approximate divertor parameters are: $n_{es} = 7 \times 10^{18}/m^3$, v_{pinch} = -9 m/s, $D_\perp$= 0.3 m^2/s, $\chi_{\perp e} = 0.8\ m^2/s$, $\chi_{\perp i} = 1.5\ m^2/s$ (all constant in flux space). No impurities. 100% recycling at the walls and target. Cryo-pump activated. Pumped neutrals are refuelled in the plasma core. A 4% target plate transmission for neutrals is assumed, allowing for the effect of slots in the MkI divertor. The pinch is employed, as diffusive perpendicular transport alone produces unreasonably broad density profiles for the high flux expansion cases of 1994/5, which parallels the modelling experience for other operational regimes on JET [8].

Table III gives comparisons among the four cases with regard to code output and experimental values for the horizontal and vertical D_α chords as well as the total target plate D_α. The ratios of recycling signals among each other for each configuration as well as the absolute values are reasonably reproduced. Renormalizing DAV in fig.2a using the predicted DAV values of table III will effect a shift of SNU points to the right and of SF points to the left, with the result that no configuration has a clear advantage in recycling levels. The code values of neutral flux to the SOL (Φ_{sol}, above the x-point) and ionizations within the separatrix (S_i) permit evaluation of the efficacy of each configuration in controlling neutral leakage to the main chamber - but, large differences for either Φ_{sol} or S_i are not predicted among the configurations.

4. Summary and Conclusions

Based on predictive EDGE2D/NIMBUS calculations, there is no indication any of the divertor equilibria of the new JET offer significant advantages over the SNU situation of 1991/2 with respect to neutral fluxes to the main SOL, or core ionizations, **for the hot-ion H-mode.** SF of 1994/5 fares least well in this sense. Thus, better R_{DD} performance likely arises largely due to the core triangularity or edge shear associated with a particular configuration rather than better recycling control, whereby these shape parameters set stability limits [3]. Recycling is clearly important in this context (fig.2c), but evidence exists there is a minium level below which high performance is no longer improved. Assisted by the cryopump, the new JET MkI divertor accesses this region (fig.2a). Finally, during the ELM-free H-mode it is observed that divertor parameters remain fairly constant after the L-H transition, attesting that the upstream SOL remains largely unaffected by core behavior until termination of the high performance phase.

5. References

[1] K. McCormick, et al., J. Nucl. Mater. **176-177** (1990) 89
[2] G.K. McCormick, Z.A. Pietrzyk et al., J. Nucl. Mater.**162-164** (1988) 264
[3] T. Hender et al., these proceedings
[4] K. Lawson, R. König et al., ibid
[5] S. Clements et al., ibid
[6] M. Erby et al., ibid
[7] A. Loarte, A. Chankin, S. Clement et al., J. Nucl. Mater. **220-222** (1995) 606
[8] A. Taroni et al., these proceedings